

Table 1 Organ weights and hemodynamics.

	(n)	BW (g)	HW (g)	HW/BW (mg/g)	HR (/min)	SBP (mm Hg)	DBP (mm Hg)
Untreated	9	28.1 ± 5.1	0.17 ± 0.02	6.12 ± 1.12	563 ± 71	94 ± 9	57 ± 6
Olmesartan	9	28.4 ± 4.6	0.14 ± 0.02*	5.17 ± 0.83*	576 ± 34	87 ± 9	53 ± 5

BW, body weight, HW, heart weight, HR, heart rate, SBP, systolic blood pressure, DBP, diastolic blood pressure. * $P < 0.05$ vs untreated group.

presence of superoxide, DHE is converted to the fluorescent molecule ethidium, which can then label nuclei by intercalating with DNA. Briefly, the unfixed frozen tissues were cut into 10 μm thick sections, and incubated with 10 μM DHE at 37 °C for 30 min in a light-protected humidified chamber. The images were obtained with a laser scanning confocal microscope. Superoxide production was demonstrated by red fluorescence labeling.

For the quantification of ethidium fluorescence from the lesions, fluorescence (intensity \times area) was measured, using the Image J in high-power ($\times 100$) images. For each vessel, total fluorescence was calculated from three to four separate fields taken in each section of the vessel to produce $n = 1$. The validity of DHE staining for the evaluation of superoxide production from the atherosclerotic lesions was already reported by us [21].

Oxidative stress evaluation

To analyze the oxidative stress overload in the aortic wall, immunohistochemistry for thioredoxin (TRX), which is a redox-active protein and considered a marker of oxidative stress, was performed as previously described [22,23]. The validity of TRX staining for the evaluation of oxidative stress in the atherosclerotic lesions was already reported by us [18].

Lipid measurement

Serum was separated by centrifugation, and stored at -80 °C. Serum total cholesterol (TC), high-density lipoprotein cholesterol (HDL-C), and triglyceride (TG) levels were measured with assay kits (Wako) according to the manufacturer's instructions. Low-density lipoprotein cholesterol (LDL-C) was calculated by the Friedewald formula.

Cytokine and TRX assays

U-937 human macrophages and thioglycolate-elicited peritoneal macrophages from apo E-deficient mice were

cultured as previously described [5], and were stimulated with 10 $\mu\text{g}/\text{ml}$ lipopolysaccharide (LPS). Olmesartan or its active metabolite RNH-6270 [5,19] was added to the cultured medium 30 min before LPS stimulation. Forty-eight hours later, interferon- γ (IFN- γ), macrophage inflammatory protein-2 (MIP-2) and TRX were assayed by enzyme-linked immunosorbent assay (ELISA) [24]. MIP-2 is thought to play an essential role in inflammatory cardiovascular diseases [25].

Statistical analysis

Values were expressed as means \pm SD. Unpaired t -test was performed. A value of $P < 0.05$ was considered statistically significant.

Results

Effects of olmesartan on organ weights and hemodynamics (Table 1)

Heart weight and heart weight to body weight ratio were significantly decreased in olmesartan group than in untreated group. Although there is a tendency for low levels of blood pressure in olmesartan group, systolic and diastolic blood pressure, and heart rate did not differ significantly between the two groups.

Effects of olmesartan on atherosclerotic lesions (Table 2, Fig. 1)

Apo E-deficient mice were kept on a cholesterol-rich diet for 8 weeks to induce fatty streak formation. The surface areas covered by fatty streak lesions were quantified in oil-red-O-stained samples, and specimens from untreated group were compared with those from olmesartan group. Untreated mice developed extensive lesions in the root of the aorta (Fig. 1). In mice treated with olmesartan, the

Table 2 Lesion area, superoxide production and oxidative stress.

	(n)	Lesion area, μm^2 (%)	Ethidium fluorescence, units	TRX expression (+1--+4) ^P
Untreated	9	59.28 \pm 21.68 $\times 10^3$ (7.64 \pm 2.78)	1.00 \pm 0.05	+++
Olmesartan	8 ^a	39.38 \pm 21.69 $\times 10^3$ (5.05 \pm 2.74)*	0.84 \pm 0.07*	+

* $P < 0.05$ vs untreated group.

^a The result of one mouse was missed due to the technical problem.

^b The degree of TRX expression was determined semi-quantitatively as previously described [22,23].

Please cite this article in press as: Shimada K, et al., Olmesartan, a novel angiotensin II type 1 receptor antagonist, reduces severity of atherosclerosis in apolipoprotein E deficient mice associated with reducing superoxide production, *Nutr Metab Cardiovasc Dis* (2010), doi:10.1016/j.numecd.2009.12.016

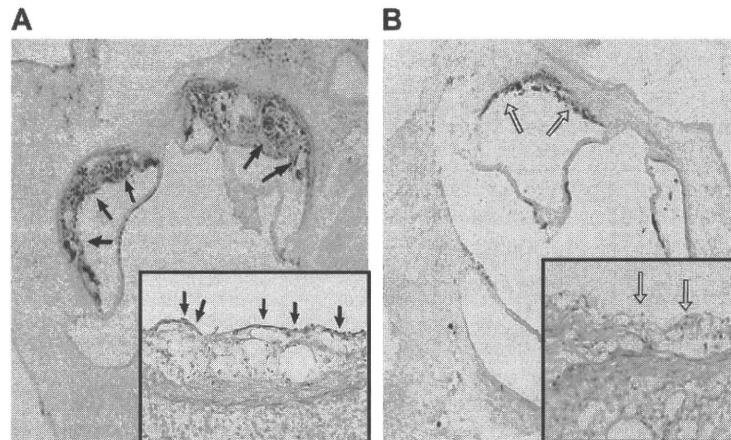


Figure 1 Effects of olmesartan on atherosclerotic lesions and oxidative stress. The lesions (white arrows) in the olmesartan-treated mouse (B) were smaller and covered less of the inner circumference of the aortic root than those (black arrows) of the olmesartan-untreated mouse (A). Insets are the expressions of thioredoxin (TRX). The expression of TRX in the lesion (white arrows) of the olmesartan-treated mouse (B) was decreased compared with that (black arrows) of the olmesartan-untreated mouse (A). Brown staining shows the positive area for TRX expression in the atherosclerotic plaques. Oil-red-O stain ($\times 50$). TRX staining ($\times 100$).

fractional area of lesions was reduced compared with the untreated mice as shown in Fig. 1.

In situ superoxide production (Table 2, Fig. 2)

In situ superoxide production was measured using DHE oxidative fluorescent microphotography. Ethidium fluorescence was detected throughout all layers of the vessel walls. Olmesartan significantly suppressed the staining of

atherosclerotic plaques (Fig. 2). Quantification of the effects of olmesartan on superoxide production was listed in Table 2.

Oxidative stress (Table 2, Fig. 1)

As shown in Fig. 1, TRX expression in the aortic wall was suppressed by olmesartan treatment compared with untreated group (Table 2, Fig. 1).

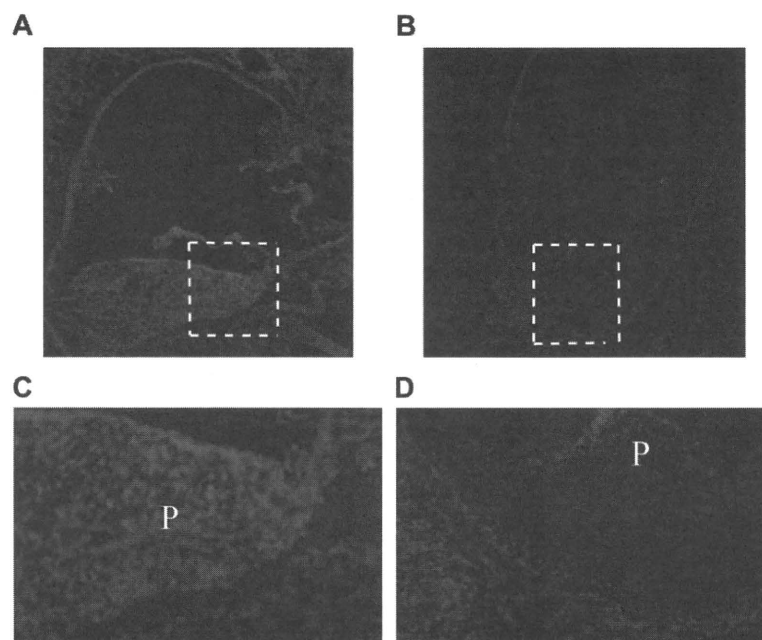


Figure 2. Representative photographs of in situ superoxide production in aortic vessel wall using dihydroethidium (DHE) staining. Treatment of olmesartan suppressed the brightness of DHE staining in vessel walls and plaques (P) in the treated mouse (B, D) compared with the untreated mouse (A, C). (C and D) are magnified pictures for dotted areas of (A and B), respectively. DHE staining (A, B $\times 10$; C, D $\times 80$).

Table 3 Lipid profiles.

	(n)	TC (mg/dl)	HDL-C (mg/dl)	LDL-C (mg/dl) ^a	TG (mg/dl)
Untreated	9	1539 ± 598	864 ± 175	669 ± 96	30 ± 53
Olmesartan	9	1449 ± 164	850 ± 104	591 ± 85	38 ± 42
					(Mn ± SD)

TC, total cholesterol, HDL-C, high-density lipoprotein cholesterol, LDL-C, low-density lipoprotein cholesterol, TG, triglyceride.

^a The values were obtained by the Friedewald formula.

Lipid profiles (Table 3)

Olmesartan treatment did not significantly modify the serum lipid profiles.

Effects of the drug on cytokine and TRX production (Table 4)

INF- γ , MIP-2 and TRX concentrations were markedly increased by LPS stimulation (Table 4). Both olmesartan and RNH-6270 suppressed LPS-induced increased cytokine production on U-937 cells and thioglycolate-elicited peritoneal macrophages in a dose-dependent manner (Table 4).

Discussion

In the current study, it was shown that olmesartan treatment suppressed the development of experimental

atherosclerosis in apo E-deficient mice associated with reducing the overload of oxidative stress and the superoxide production of aortic walls without significant hemodynamic changes. The in vitro study actually showed that both olmesartan and its active metabolite RNH-6270, an enantiomer of olmesartan, suppressed INF- γ , MIP-2 and TRX production in cultured cells. Accordingly, the in vitro data may support the anti-atherosclerotic effects of the drugs in vivo.

Chronic inflammation is thought to be of central importance in atherosclerosis [1,26]. It was shown that regular and chronic exercise could suppress overt and subclinical inflammation [27,28]. We and other investigators had already reported that experimental atherosclerosis in apo E-deficient mice was markedly suppressed by Fc γ portion of immunoglobulin administration possibly by an anti-inflammatory action via inhibitory Fc γ receptor IIB [29–31].

There is also increasing evidence to support the critical role of both free radicals and oxidative stress in the

Table 4 Effects of olmesartan and RNH-6270 on cytokine production in vitro.

LPS (10 μ g/ml)	Conditions		Cytokines concentrations		
	Olmesartan (pg)	RNH-6270 (pg)	INF- γ (pg/ml)	MIP-2 (ng/ml)	TRX (ng/ml)
U-937 cells					
–	–	–	1.4 ± 0.5	8 ± 3	10 ± 4
+	–	–	3.9 ± 1.1	45 ± 15	34 ± 5
+	1	–	3.4 ± 0.5	32 ± 5	30 ± 8
+	10	–	2.3 ± 0.6*	21 ± 10*	20 ± 8*
+	100	–	2.0 ± 0.4*	10 ± 7**	12 ± 5**
–	–	–	1.5 ± 0.5	5 ± 4	13 ± 5
+	–	–	4.5 ± 0.8	52 ± 15	29 ± 6
+	–	1	4.0 ± 1.0	45 ± 11	25 ± 5
+	–	10	3.2 ± 0.8	34 ± 8	15 ± 5*
+	–	100	2.2 ± 0.4**	16 ± 7**	15 ± 6*
Peritoneal macrophages					
–	–	–	3.6 ± 1.5	10 ± 5	–
+	–	–	6.0 ± 0.5	98 ± 21	–
+	1	–	5.2 ± 1.0	74 ± 15	–
+	10	–	4.1 ± 0.7*	56 ± 20*	–
+	100	–	3.5 ± 1.0*	52 ± 24*	–
–	–	–	3.0 ± 2.1	12 ± 6	–
+	–	–	7.1 ± 1.4	104 ± 15	–
+	–	1	5.0 ± 1.5	77 ± 25	–
+	–	10	4.7 ± 0.9*	68 ± 30	–
+	–	100	4.5 ± 1.2*	55 ± 20*	–
					(Mn ± SD)

INF- γ , interferon- γ , MIP-2, macrophage inflammatory protein-2, TRX, thioredoxin. Each value was derived from 4 to 6 trials. Cell viability in each experiment was more than 93% by trypan blue exclusion test. * $P < 0.05$; ** $P < 0.01$ vs olmesartan (–) or RNH-6270 (–) conditions.

development of atherosclerosis [20,32–34]. We had already demonstrated that MCI-186, a free radical scavenger, suppressed the severity of experimental atherosclerosis [18]. The AT₁ receptor antagonist such as olmesartan is reported to suppress not only cytokine production but also free radical production in addition to its hemodynamic effects [5–7]. Indeed, angiotensin stimulation has been reported to produce free radicals from various cells [35–37]. Free radicals from vessel walls are thought to play critical roles in atherogenesis. Free radicals induce the expression of adhesion molecules and chemokines, accelerate atherosclerotic plaque formation, increase matrix metalloprotease production, and cause vulnerable plaques [38]. Recent studies suggested that olmesartan attenuates experimental atherosclerosis via an anti-oxidative action, prevention of endothelial disruption, and the decrease of macrophage accumulation in the lesions [8–13,39].

In the present study, we clearly demonstrated that olmesartan suppressed the overload of free radicals in aortic walls assessed by DHE staining [7,20,21] and TRX expression [18,22,23]. Immunohistochemical study showed that the intensity of both DHE staining and TRX staining in the aortic wall was reduced by olmesartan treatment compared with untreated group. It has already been established that the degree of tissue TRX staining correlates with the overload of oxidative stress [18,22,23]. Thus, the decrease of the intensity of both DHE staining and TRX expression in aortic walls may reflect the decrease of oxidative stress by olmesartan treatment.

In addition, *in vitro* study showed that both olmesartan and its active metabolite RNH-6270 suppressed IFN- γ , MIP-2 and TRX production. Although there were no significant differences in serum cytokines (interleukin-1 β and IFN- γ) between olmesartan-treated and -untreated mice *in vivo* (data not shown), these *in vitro* results may suggest that beneficial effects of olmesartan in apo E-deficient mice is partly due to the suppression of inflammatory events in the vessel walls. The *in vitro* data may well explain the anti-atherosclerotic effects of olmesartan *in vivo*.

It is now well recognized that vascular AT₁ receptor stimulated superoxide production is NAD(P)H oxidase-dependent. However, in the current study, the aortic NAD(P)H oxidase activity with and without olmesartan treatment was not examined.

We used this dosage of the drug to avoid the effect of the drug-induced hypotension. Indeed, the drug did not exhibit the lowering effects of systolic blood pressure significantly. At present time, we have no answers whether the suppressive effects of olmesartan for oxidative stress is dependent of blood pressure lowering effect or not, because angiotensin II-mediated hypertension is associated with the increased oxidative stress [32–34].

Novel findings of the current study compared with the previous work [8–13,16,39,40] are that olmesartan inhibits experimental atherosclerosis in apo E-deficient mice without significant hemodynamic changes, that is, the drug has the potential to reduce atherosclerosis not by lowering blood pressure, and that the effects were associated with reduced superoxide production and oxidative stress even with hyperlipidemic state. It was also shown in the current study that the capability of the active metabolite RNH-6270

to reduce inflammation was demonstrated. Accordingly, olmesartan may be beneficial for atherosclerotic patients associated with reducing oxidative stress. In conclusion, inhibition of free radical production and oxidative stress may be one mechanism by which olmesartan decreases the severity of experimental atherosclerosis in apo E-deficient mice. Our results suggest that more widespread clinical use of the drug for atherosclerotic patients might be warranted.

Conflict of interest

The authors have no conflict of interest.

References

- [1] Ross R. Atherosclerosis: an inflammatory disease. *N Engl J Med* 1999;340:115–26.
- [2] Burnier M. Angiotensin II type 1 receptor blockers. *Circulation* 2001;103:904–12.
- [3] Mollnau H, Wendt M, Szöcs K, Lassègue B, Schulz E, Oelze M, et al. Effects of angiotensin II infusion on the expression and function of NAD(P)H oxidase and components of nitric oxide/cGMP signaling. *Circ Res* 2002;90:e58–65.
- [4] Warnholtz A, Nickenig G, Schulz E, Macharzina R, Bräsen JH, Skatchkov M, et al. Increased NADH-oxidase-mediated superoxide production in the early stages of atherosclerosis. Evidence for involvement of the renin-angiotensin system. *Circulation* 1999;99:2027–33.
- [5] Yuan Z, Nimata M, Okabe TA, Shioji K, Hasegawa K, Kita T, et al. Olmesartan, a novel AT₁ antagonist, suppresses cytotoxic myocardial injury in autoimmune heart failure. *Am J Physiol Heart Circ Physiol* 2005;289:H 1147–52.
- [6] Weinstock JV, Blum AM, Kassab JT. Angiotensin II is chemotactic, for a T-cell subset which can express migration factor activity in murine *Schistosomiasis mansoni*. *Cell Immunol* 1987;107:180–7.
- [7] Takaya T, Kawashima S, Shinohara M, Yamashita T, Toh R, Sasaki N, et al. Angiotensin II type 1 receptor blocker telmisartan suppresses superoxide production and reduces atherosclerotic lesion formation in apolipoprotein E-deficient mice. *Atherosclerosis* 2006;186:402–10.
- [8] van der Hoorn JM, Kleemann R, Havekes LM, Kooistra T, Princen HM, Jukema JW. Olmesartan and pravastatin additively reduce development of atherosclerosis in APOE*3 Leiden transgenic mice. *J Hypertens* 2007;25:2454–62.
- [9] Arishiro K, Hoshiga M, Negoro N, Jin D, Takai S, Miyazaki M, et al. Angiotensin receptor-1 blocker inhibits atherosclerotic changes and endothelial disruption of the aortic valve in hypercholesterolemic rabbits. *J Am Coll Cardiol* 2007;49:1482–9.
- [10] Kurata A, Nishizawa H, Kihara S, Maeda N, Sonoda M, Okada T, et al. Blockade of Angiotensin II type-1 receptor reduces oxidative stress in adipose tissue and ameliorates adipocytokine dysregulation. *Kidney Int* 2006;70:1717–24.
- [11] Takai S, Jin D, Sakaguchi M, Muramatsu M, Miyazaki M. The regressive effect of an angiotensin II receptor blocker on formed fatty streaks in monkeys fed a high-cholesterol diet. *J Hypertens* 2005;23:1879–86.
- [12] Suzuki J, Iwai M, Li Z, Li JM, Min LJ, Ide A, et al. Effect of combination of calcium antagonist, azelmidipine, and AT₁ receptor blocker, olmesartan, on atherosclerosis in apolipoprotein E-deficient mice. *J Hypertens* 2005;23:1383–9.
- [13] Ferrario CM. Use of angiotensin II receptor blockers in animal models of atherosclerosis. *Am J Hypertens* 2002;15:95–135.
- [14] Plump AS, Smith JD, Hayek T, Aalto-Setälä K, Walsh A, Verstuyft JG, et al. Severe hypercholesterolemia and

- atherosclerosis in apolipoprotein E-deficient mice created by homologous recombination in ES cells. *Cell* 1992;71:343–53.
- [15] Nakashima Y, Plump AS, Raines EW, Breslow JL, Ross R. ApoE-deficient mice develop lesions of all phases of atherosclerosis throughout the arterial tree. *Arterioscler Thromb* 1994;14:133–40.
- [16] Kato M, Sada T, Chuma H, Mizuno M, Terashima H, Fukushima Y, et al. Severity of hyperlipidemia does not affect antiatherosclerotic effect of an angiotensin II receptor antagonist apolipoprotein E-deficient mice. *J Cardiovasc Pharmacol* 2006;47:764–9.
- [17] Murayama T, Yokode M, Kataoka H, Imabayashi T, Yoshida H, Sano H, et al. Intraperitoneal administration of anti-c-fms monoclonal antibody prevents initial events of atherogenesis but does not reduce the size of advanced lesions in apolipoprotein E-deficient mice. *Circulation* 1999;99:1740–6.
- [18] Okabe T, Kishimoto C, Shimada K, Murayama T, Yokode M, Kita T. Effects of MCI-186 (Edaravone), a novel free radical scavenger, upon experimental atherosclerosis in apolipoprotein E-deficient mice. *Circ J* 2006;70:1216–9.
- [19] Mizuno M, Sada T, Ikeda M, Fukuda N, Miyamoto M, Yanagisawa H, et al. Pharmacology of CS-866, a novel non-peptide angiotensin II receptor antagonist. *Eur J Pharmacol* 1995;285:181–8.
- [20] Miller FJ, GuHerman DD, Rios CD, Heistad DD, Davidson BL. Superoxide production in vascular smooth muscle contributes to oxidative stress and impaired relaxation in atherosclerosis. *Circ Res* 1998;82:1298–305.
- [21] Shimada K, Murayama T, Yokode M, Kita T, Uzui H, Ueda T, et al. N-acetylcysteine reduces the severity of atherosclerosis in apolipoprotein E deficient mice via reducing superoxide production. *Circ J* 2008;73:1337–41.
- [22] Shioji K, Kishimoto C, Nakamura H, Masutani H, Yuan Z, Oka S, et al. Overexpression of thioredoxin-1 in transgenic mice attenuates adriamycin-induced cardiotoxicity. *Circulation* 2002;106:1403–9.
- [23] Miyamoto M, Kishimoto C, Shioji K, Nakamura H, Toyokuni S, Nakayama Y, et al. Difference in thioredoxin expression in viral myocarditis in inbred strains of mice. *Jpn Circ J* 2001;65:561–4.
- [24] Kishimoto C, Shioji K, Nakamura H, Nakayama Y, Yodoi J, Sasayama S. Serum thioredoxin (TRX) levels in patients with heart failure. *Jpn Circ J* 2001;65:491–4.
- [25] Kishimoto C, Kawamata H, Sakai S, Shinohara H, Ochiai H. Role of MIP-2 in coxsackie virus B3 myocarditis. *J Mol Cell Cardiol* 2000;32:631–8.
- [26] Kondo N, Nomura M, Nakaya Y, Ito S, Ohguro T. Association of inflammatory marker and highly sensitive C-reactive protein with aerobic exercise capacity, maximum oxygen uptake and insulin resistance in healthy middle-aged volunteers. *Circ J* 2005;69:452–7.
- [27] Gielen S, Adams V, Möbius-Winkler S, Linke A, Erbs S, Yu J, et al. Anti-inflammatory effects of exercise training in the skeletal muscle of patients with chronic heart failure. *J Am Coll Cardiol* 2003;42:869–72.
- [28] Milani RV, Lavie CJ, Mehra MR. Reduction in C-reactive protein through cardiac rehabilitation and exercise training. *J Am Coll Cardiol* 2004;43:1056–61.
- [29] Yuan Z, Kishimoto C, Sano H, Shioji K, Xu Y, Yokode M. Immunoglobulin treatment suppresses atherosclerosis in apolipoprotein E-deficient mice via the Fc portion. *Am J Physiol* 2003;285:H899–906.
- [30] Shioji K, Kishimoto C, Sasayama S. Fc receptor-mediated inhibitory effect of immunoglobulin therapy on autoimmune giant cell myocarditis: concomitant suppression of the expression of dendritic cells. *Circ Res* 2001;89:540–6.
- [31] Nicoletti A, Kaveri S, Caligiuri G, Bariéty J, Hansson GK. Immunoglobulin treatment reduces atherosclerosis in apo E knockout mice. *J Clin Invest* 1998;102:910–8.
- [32] Parthasarathy S, Santanam N, Ramachandran S, Meilhac O. Oxidants and antioxidants in atherogenesis: an appraisal. *J Lipid Res* 1999;40:2143–57.
- [33] Bernal-Mizrachi C, Gates AC, Weng S, Imamura T, Knutsen RH, DeSantis P, et al. Vascular respiratory uncoupling increases blood pressure and atherosclerosis. *Nature* 2005;435:502–6.
- [34] Franzoni F, Ghiadoni L, Galetta F, Plantinga Y, Lubrano V, Huang Y, et al. Physical activity, plasma antioxidant capacity, and endothelium-dependent vasodilation in young and older men. *Am J Hypertens* 2005;18:510–6.
- [35] Zhang H, Schmeisser A, Garlachs CD, Plötze K, Damme U, Mügge A, et al. Angiotensin II-induced superoxide anion generation in human vascular endothelial cells: role of membrane-bound NADH/NADPH-oxidases. *Cardiovasc Res* 1999;44:215–22.
- [36] Sorescu D, Weiss D, Lassègue B, Clempus RE, Szöcs K, Sorescu GP, et al. Superoxide production and expression of nox family proteins in human atherosclerosis. *Circulation* 2002;105:1429–35.
- [37] Cathcart MK. Regulation of superoxide anion production by NADPH oxidase in monocytes/macrophages: contributions to atherosclerosis. *Arterioscler Thromb Vasc Biol* 2004;24:23–8.
- [38] Rajagopalan S, Meng XP, Ramasamy S, Harrison DG, Galis ZS. Reactive oxygen species produced by macrophage-derived foam cells regulate the activity of vascular matrix metalloproteinases in vitro. Implications for atherosclerotic plaque stability. *J Clin Invest* 1996;98:2572–9.
- [39] Tsuda M, Iwai M, Li JM, Li HS, Min LJ, Ide A, et al. Inhibitory effects of AT₁ receptor blocker, olmesartan, and estrogen on atherosclerosis via anti-oxidative stress. *Hypertension* 2005;45:545–51.
- [40] Ni W, Kitamoto S, Ishibashi M, Usui M, Inoue S, Hiasa K, et al. Monocyte chemoattractant protein-1 is an essential inflammatory mediator in angiotensin II-induced progression of established atherosclerosis in hypercholesterolemic mice. *Arterioscler Thromb Vasc Biol* 2004;24:534–9.

MicroRNA-33 encoded by an intron of sterol regulatory element-binding protein 2 (*Srebp2*) regulates HDL in vivo

Takahiro Horie^{a,b}, Koh Ono^{a,1}, Masahito Horiguchi^a, Hitoo Nishi^a, Tomoyuki Nakamura^c, Kazuya Nagao^a, Minako Kinoshita^a, Yasuhide Kuwabara^a, Hiroyuki Marusawa^d, Yoshitaka Iwanaga^e, Koji Hasegawa^f, Masayuki Yokode^b, Takeshi Kimura^a, and Toru Kita^g

^aDepartment of Cardiovascular Medicine, Graduate School of Medicine, Kyoto University, Kyoto 606-8507, Japan; ^bDepartment of Clinical Innovative Medicine, Translational Research Center, Graduate School of Medicine, Kyoto University, Kyoto 606-8507, Japan; ^cDepartment of Pharmacology, Kansai Medical University, Moriguchi, Osaka 570-8506, Japan; ^dDepartment of Gastrointestinal Medicine, Graduate School of Medicine, Kyoto University, Kyoto 606-8507, Japan; ^eDivision of Cardiology, Department of Internal Medicine, School of Medicine, Kinki University, Osaka 589-8511, Japan; ^fDivision of Translational Research, Clinical Research Institute, Kyoto Medical Center, Kyoto 612-8555, Japan; and ^gDepartment of Cardiovascular Medicine, Kobe City General Hospital, Kobe 650-0046, Japan

Edited by Jan L. Breslow, Rockefeller University, New York, NY, and approved August 24, 2010 (received for review June 16, 2010)

Sterol regulatory element-binding protein 2 (SREBP-2) transcription factor has been identified as a key protein in cholesterol metabolism through the transactivation of the LDL receptor and cholesterol biosynthesis genes. Here, we generated mice lacking microRNA (miR)-33, encoded by an intron of the *Srebp2*, and showed that miR-33 repressed the expression of ATP-binding cassette transporter A1 (ABCA1) protein, a key regulator of HDL synthesis by mediating cholesterol efflux from cells to apolipoprotein A (apoA)-I. In fact, peritoneal macrophages derived from miR-33-deficient mice showed a marked increase in ABCA1 levels and higher apoA-I-dependent cholesterol efflux than those from WT mice. ABCA1 protein levels in liver were also higher in miR-33-deficient mice than in WT mice. Moreover, miR-33-deficient mice had significantly higher serum HDL cholesterol levels than WT mice. These data establish a critical role for miR-33 in the regulation of ABCA1 expression and HDL biogenesis in vivo.

ABCA1 | macrophage | cholesterol efflux | liver | metabolic syndrome

ATP-binding cassette transporter A1 (ABCA1), a 254-kDa cytoplasmic membrane protein, is a pivotal regulator of lipid efflux from cells to apolipoproteins (1). ABCA1 mediates the rate-controlling step in HDL particle formation and plays an important role in reverse cholesterol transfer (2, 3). Mutations in the ABCA1 gene cause Tangier disease, which is characterized by the near absence of plasma HDL cholesterol associated with storage of cholesterol esters in reticuloendothelial tissues (4–7). *Abca1* mRNA and protein are very unstable, with a half life of 1–2 h in murine macrophages (8), which indicates that new transcription and translation are major factors in ensuring constant and inducible ABCA1 expression.

Sterol regulatory element-binding proteins (SREBPs), including SREBP-1a, -1c, and -2, modulate the transcription of a number of genes involved in the synthesis and receptor-mediated uptake of cholesterol and fatty acids (9–11). In sterol-depleted cells, SREBPs are cleaved by proteases in the Golgi, releasing the N-termini, which translocate into the nucleus and bind to SREs in the enhancers of multiple genes encoding enzymes and proteins involved in cholesterol biosynthesis and lipid uptake (11–13). Results to date support the notion that SREBP-1 primarily activates the fatty acid triglyceride and phospholipid pathways, whereas SREBP-2 is the prominent isoform for cholesterol synthesis and uptake (9, 10, 12).

MicroRNAs (miRs) are small, non-protein-coding RNAs that base pair with specific mRNAs and inhibit translation or promote mRNA degradation. Recent reports have indicated that miR-33 controls cholesterol homeostasis based on knockdown experiments using antisense technology (14–16). Antisense inhibition of

miRNA function has been an important tool for elucidating miRNA biology. However, to determine the potential developmental function of specific miRNAs and to perform longer-term studies, it is necessary to generate mice lacking each miRNA. We generated miR-33-deficient mice, which were born at the expected Mendelian ratio, and show here that miR-33, encoded by an intron 16 of the *Srebp2* gene, repressed the ABCA1 protein, which resulted in a reduction in HDL concentration.

Results

miR-33 Is Encoded by Intron 16 of the Human, Mouse, Cow, and Chicken SREBP2 Genes and Targets ABCA1. miR-33 is encoded by intron 16 of the human, mouse, cow, chicken *SREBP2* genes. The sequence of miR-33 is identical, and the stem-loop pre-miRNA is highly conserved in mammals (Fig. 1A). We searched for potential target genes of miR-33 in a public database (TargetScan, <http://www.targetscan.org/>), and found that three putative miR-33 binding sites existed in the 3'-untranslated region (UTR) of the *ABCA1* mRNA, and that this region was evolutionarily conserved (Fig. 1A). To test whether the putative miR-33 target sequence in the *Abca1* 3'-UTR could mediate translational repression, we inserted the 3'-UTR of the *Abca1* transcript into a luciferase expression plasmid (*luc-Abca1* 3'-UTR), which we transfected into HEK 293T cells. CMV-driven miR-33 resulted in a decrease in luciferase activity compared with miR-146a or control vector (miR-control). Mutation in the potential binding site in the 3'-UTR abolished the effect of miR-33 (Fig. 1B). Next, we transduced miR-33 into a monocytic cell line, THP-1, and a human primary hepatocyte cell line, HuS-E/2 (17), using lentivirus. The transfection efficiency of the lentivirus was always more than 90% (Fig. S1A and B). Overexpression of miR-33 resulted in a decrease in ABCA1 protein expression compared with the control vector in both cell lines (Fig. 1C). Because ABCA1 mediates cholesterol efflux from macrophages to lipid-free apoA-I (3), we further examined cholesterol efflux from THP-1-derived macrophages, which were differentiated from THP-1 by stimulation with phorbol 12-myristate 13 acetate (PMA) (100 nM) for 3 d. As shown in Fig. 1D, apoA-I-mediated chole-

Author contributions: T.H., K.O. and T. Kita designed research; T.H., M.H., H.N., K.N., M.K., and Y.K. performed research; M.H., T.N., and H.M. contributed new reagents/analytic tools; T.H., K.O., T.N., Y.L., K.H., M.Y., T. Kimura, and T. Kita analyzed data; and T.H. and K.O. wrote the paper.

The authors declare no conflict of interest.

This article is a PNAS Direct Submission.

Freely available online through the PNAS open access option.

¹To whom correspondence should be addressed. E-mail: kohono@kuhp.kyoto-u.ac.jp.

This article contains supporting information online at www.pnas.org/lookup/suppl/doi:10.1073/pnas.1008499107/-DCSupplemental.

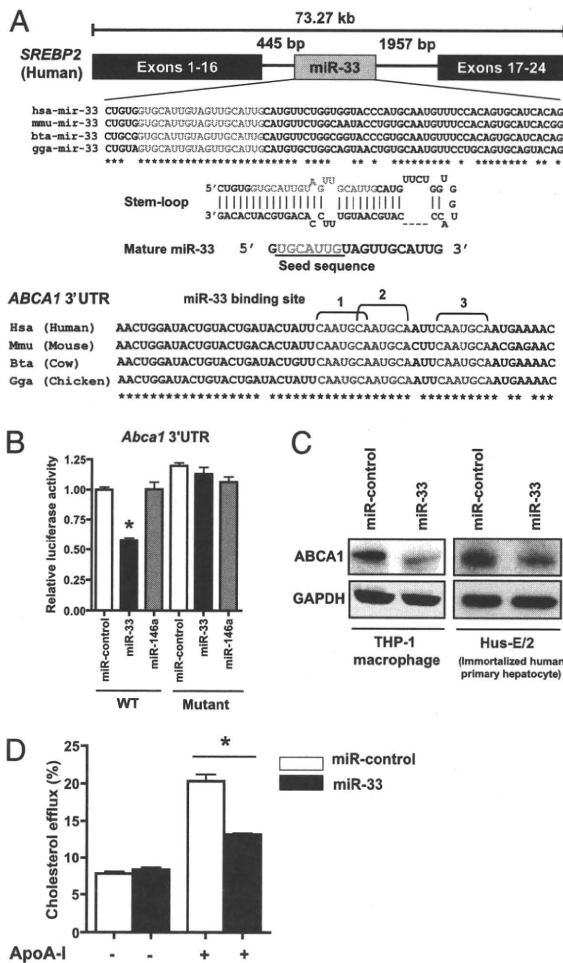


Fig. 1. ABCA1 is a target of miR-33. (A) Schema and sequence alignment of *SREBP2*, miR-33, and *ABCA1* 3' UTR. miR-33 is located in intron16 of *SREBP2*. There are three potential conserved miR-33 binding sites in the *ABCA1* 3' UTR. (B) 293T cells were transfected with WT or mutant *Abca1* 3' UTR luciferase constructs, along with expression plasmids for miR-control (negative control), miR-33, and miR-146a. Values are the means \pm SE of four independent experiments. * $P < 0.01$ compared with other columns. (C) Western blot analysis of ABCA1 in THP-1-derived macrophages and Hus-E/2 (human primary hepatocytes) transfected with miR-control and miR-33, using a lentivirus vector. (D) Cholesterol efflux was measured in the presence or absence of apoA-I (15 μ g/mL) for 24 h in THP-1-derived macrophages transfected with miR-control and miR-33. Values are the means \pm SE of three independent experiments. * $P < 0.01$.

sterol efflux was significantly reduced in miR-33 transduced macrophages compared with miR-control transduced cells.

miR-33 Is Expressed with *Srebp2*. We next confirmed that intronic miR-33, expressed synchronously with *Srebp2*, is spliced to target ABCA1. We amplified genomic DNA and cDNA fragments of the mouse *Srebp2* gene that cover the 5' end of exon 16 and 3' end of exon 17, and cloned them into a pcDNA3.1 vector, to make minigenes that contain exon 16–intron 16–exon 17 and exon 16–exon 17 (Fig. 2A). As shown by RT-PCR, intron 16 was spliced out of the transcript of exon 16–intron 16–exon 17 in HEK 293T cells (Fig. 2B). This *Srebp2* exon 16–intron 16–exon 17 minigene significantly suppressed luciferase activity in 293T cells transfected with a luc-*Abca1* 3'-UTR construct compared with the *Srebp2* exon 16–exon 17 minigene and pcDNA3.1 empty vector (Fig. 2C). Transfection of

the *Srebp2* exon 16–intron 16–exon 17 minigene also resulted in a decrease in ABCA1 protein levels compared with the *Srebp2* exon 16–exon 17 minigene and pcDNA3.1 empty vector in THP-1 cells (Fig. 2D). These experiments suggested that intronic miR-33 is typically and coordinately expressed with its host gene, as reported for other intronic miRNAs (18, 19).

Sterol Depletion Activated *SREBP2* and Increased miR-33 Expression.

To study the relevance of the miR-33/*SREBP2*/*ABCA1* cholesterol regulatory circuit, we cultured THP-1 cells under sterol-depleted conditions by the removal of serum from the culture media (SFM) or in the presence of statin. Under these conditions, THP-1 cells had normal morphology, and no cell death was detected. As shown in Fig. 3A, SFM decreased ABCA1 protein levels in THP-1 cells in a time-dependent manner. *LDL-receptor* and *SREBP2* mRNA expression levels increased in a time-dependent manner after serum depletion (Fig. 3B and C). Expression of miR-33 paralleled *SREBP2* expression (Fig. 3D). The same experiment was conducted in cells treated with simvastatin. Simvastatin reduced the expression of ABCA1 in a dose- and time-dependent manner (Fig. S2A and B). The expression levels of *LDL-receptor*, *SREBP2*, and miR-33 increased in time-dependent manners as in SFM (Fig. S2C–E). We further suppressed endogenous miR-33 in THP-1-derived macrophages by the transduction of a “decoy” gene, which contained 9-tandem repeats of antisense sequences against miR-33 downstream of the luciferase gene (Fig. S3A). Overexpression of miR-33 along with this decoy gene significantly suppressed luciferase activity (Fig. S3B). The suppression of ABCA1 protein levels in response to sterol depletion was reversed by the miR-33 decoy gene (Fig. S3C), which was consistent with the notion that miR-33 mediates cholesterol-regulated posttranscriptional control of ABCA1 levels.

Generation of miR-33-Deficient Mice. We deleted the region that encodes the complete premiRNA sequence of miR-33 by introducing loxP sites for Cre-mediated recombination into intron 16 of the mouse *Srebp2* (Fig. 4A–C). Because disruption of the *Srebp2* causes embryonic lethality (20), it was important that the miR-33 targeting strategy did not alter *Srebp2* transcription or splicing. Deletion of miR-33 did not alter the expression of *SREBP2* protein (Fig. 4D) or interfere with *Srebp2* mRNA splicing and expression (Fig. 4E and Fig. S4) in miR-33-deficient mice. *Srebp2* mRNA splicing and expression were not altered even at later time points (Fig. S5). Relative expression levels of miR-33 and *Srebp2* are shown in Fig. S6A. miR-33 appears to be coexpressed with the *Srebp2* host gene as seen in THP-1 cells (Fig. 3). Loss of miR-33 expression in these mice was confirmed in the liver (Fig. 4F) and in other organs (Fig. S6B and C) by real-time PCR. Mice homozygous for the miR-33 deletion were born at the expected Mendelian ratio, were viable, fertile, and did not display obvious abnormalities in size, shape, or structure up to 16 wk of age.

miR-33 Deficiency Enhances Cholesterol Efflux in Macrophages. To investigate the role of miR-33 in mice, we first compared the function of peritoneal macrophages in WT and miR-33-deficient mice. ABCA1 protein expression levels were considerably higher in macrophages of miR-33-deficient mice than those of WT mice (Fig. 5A). We measured apoA-I-mediated cholesterol efflux from peritoneal macrophages and found that macrophages in miR-33-deficient mice had higher apoA-I-mediated cholesterol efflux than WT mice (Fig. 5B).

miR-33 Deletion Enhances HDL Levels. Overexpression of hepatic ABCA1 raises HDL cholesterol levels (21), and liver-specific deletion of ABCA1 results in a substantial ($\approx 80\%$) decrease in plasma HDL cholesterol in chow-fed mice (22). Therefore, we measured ABCA1 protein expression levels in the liver. Fig. 5C and D indicate that ABCA1 protein levels were higher in miR-33-deficient mice liver than in WT mice liver of both sexes. High-performance

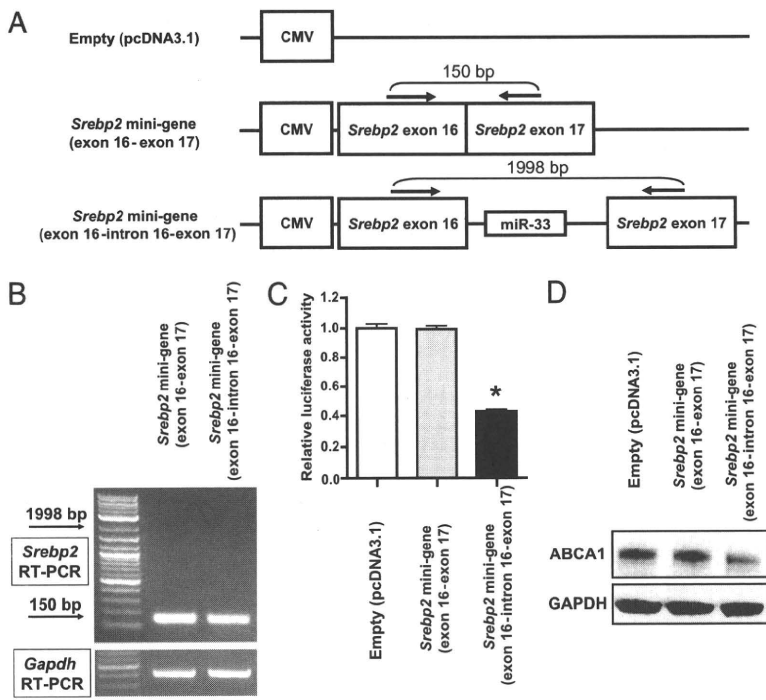


Fig. 2. Analysis using *Srebp2* minigene. (A) Schema of *Srebp2* minigene used in this report. Arrows indicate RT primers. (B) RT-PCR analysis of 293T cells transfected with *Srebp2* minigene. Note that there is no band around 2,000 bp, indicating that intron 16 was correctly spliced. (C) 293T cells were transfected with WT *Abca1* 3'UTR luciferase construct, along with expression plasmids. Values are means \pm SE of four independent experiments. * $P < 0.05$ compared with empty vector (pcDNA3.1) or the *Srebp2* minigene (exon 16–exon 17). (D) Western blot analysis of ABCA1 in THP-1 macrophages transfected with the *Srebp2* minigene using lentivirus vectors. GAPDH was used as a loading control.

liquid chromatography (HPLC) with gel permeation columns was used for classifying and quantifying lipoproteins on the basis of differences of particle size (23, 24). Fig. 5 *E* and *F* shows representative results of the HPLC elution profile of serum from WT (black) and miR-33-deficient mice (red) at the age of 16 wk. HDL from miR-33-deficient mice showed a broader peak with a slight shift to the left consistent with cholesterol enrichment. Serum lipid profiles of mice at the age of 16 wk are summarized in Table 1. miR-33-deficient mice had significantly higher total cholesterol and HDL cholesterol levels than WT mice, whereas triglyceride levels were unchanged. Elevation of HDL was prominent in female mice. In fact, the expression level of miR-33 showed an ≈ 1.5 -fold increase in the liver of WT female mice compared with WT male mice (Fig. S6*D*). Moreover, the increased levels of HDL were composed mainly of very large, large, and medium HDL (mature HDL). Because *Abcg1*, which is required for cholesterol efflux to HDL and contributes to form mature HDL,

is a potential target of miR-33 in rodents (not humans) (14, 16) (Fig. S7*A*), we also inserted the 3'-UTR of the *Abcg1* transcript into a luciferase expression plasmid (*luc-Abcg1* 3'-UTR). CMV-driven miR-33 resulted in a decrease in luciferase activity compared with miR-146a or control vector (miR-control) in HEK 293T cells. Mutation in the potential binding site in the 3'-UTR abolished the effect of miR-33 (Fig. S7*B*). We further measured the protein levels of ABCG1 in liver. However, the levels were the same in WT and miR-33-deficient mice of both sexes (Fig. S7*C* and *D*).

Discussion

Recent studies have shown that miR-33 helps to regulate the homeostasis of HDL cholesterol, suggesting that it might be a possible target for the treatment of cardiovascular and metabolic disorders (14–16), which reported similar or complementary findings. Expression of miR-33 was found in various cells and tissues, including

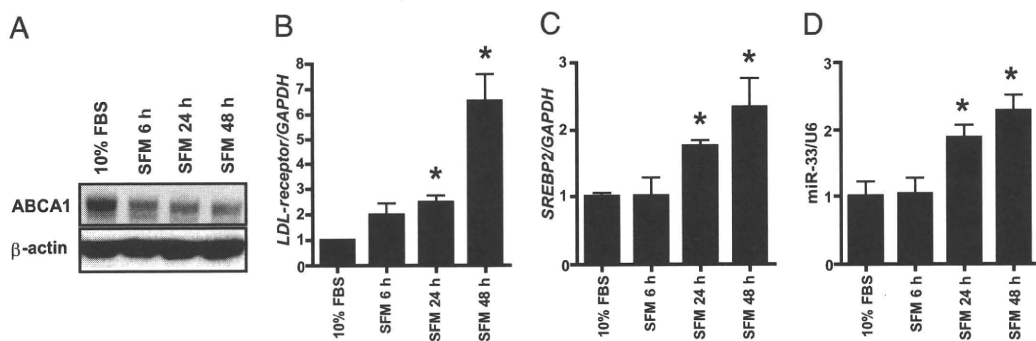


Fig. 3. Effect of serum starvation in THP-1 macrophages. (A) Western blot analysis of ABCA1 protein levels under serum starvation conditions for the indicated time periods in THP-1 macrophages. GAPDH was used as a loading control. (B) Quantitative real-time PCR analysis of *LDL receptor* expression levels under serum starvation conditions for the indicated time periods in THP-1 macrophages. Values are mean \pm SE of six independent experiments with normalization using *GAPDH* expression. * $P < 0.05$ compared with 10% FBS. (C) Quantitative real-time PCR analysis of *SREBP2* expression levels under serum starvation conditions for the indicated time periods in THP-1 macrophages. Values are mean \pm SE of six independent experiments with normalization using *GAPDH* expression. * $P < 0.05$ compared with 10% FBS. (D) Quantitative real-time PCR analysis of miR-33 under serum starvation conditions for the indicated time periods in THP-1 macrophages. Values are mean \pm SE of six independent experiments with normalization using U6 snRNA. * $P < 0.05$ compared with 10% FBS.

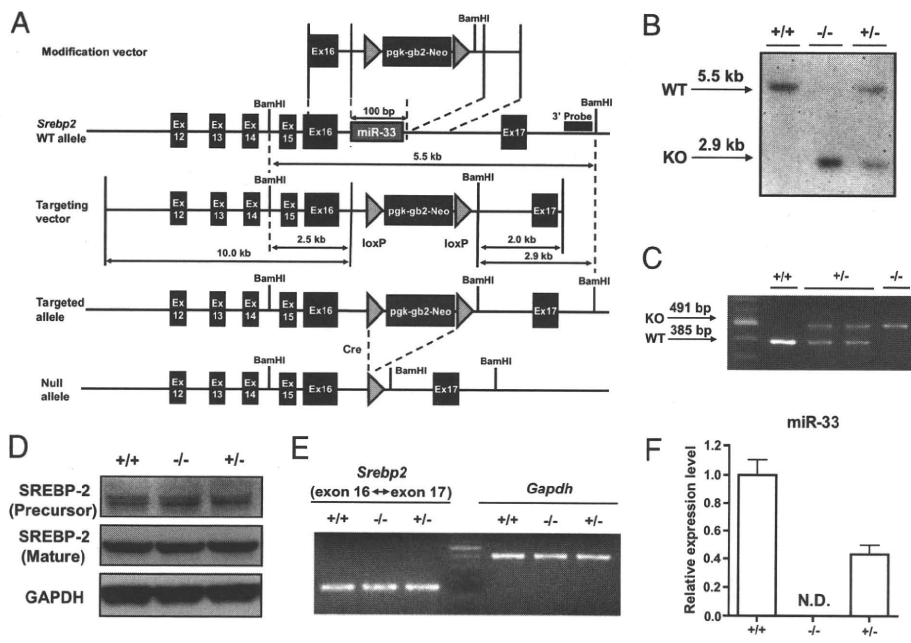


Fig. 4. Generation of miR-33-deficient mice. (A) Strategy to generate miR-33-deficient mice by homologous recombination. The premiR-33 sequence was replaced with a neomycin resistance cassette (pgk-gb2-Neo) flanked by loxP sites. The neomycin resistance cassette was removed in the mouse germ line by breeding heterozygous mice with *Ayu-1* Cre mice, which express Cre recombinase in multiple tissues, including the germ line. (B) Southern blotting of mouse tail genome. (C) PCR analysis of mouse tail genome. (D) Western blot analysis of SREBP-2 in the liver of 8-wk-old male mice (precursor, 126 kDa; mature, 55 kDa). GAPDH was used as a loading control. (E) RT-PCR analysis of *Srebp2* in liver of 8-wk-old male mice. Sense primer was designed in exon 16 of *Srebp2*, and antisense primer was designed in exon 17 of *Srebp2*. *Gapdh* was used as control. (F) Quantitative real-time PCR analysis of miR-33 in liver of 8-wk-old male mice, using a Taqman microRNA assay. N.D., not determined.

macrophages, hepatic cells, endothelial cells, brain, liver, colon, small intestine, and skeletal muscle. The predominant target identified for miR-33 was the gene encoding *ABCA1*. It was suggested that miR-33 antisense approaches resulted in augmented

HDL-cholesterol levels in mice. One report indicated that three injections of locked nucleic acid (LNA) antisense over 5 d elevated plasma HDL-cholesterol levels by $\approx 35\%$, with only modest effects of miR-33a LNA-antimiR on hepatic *ABCA1* mRNA/protein

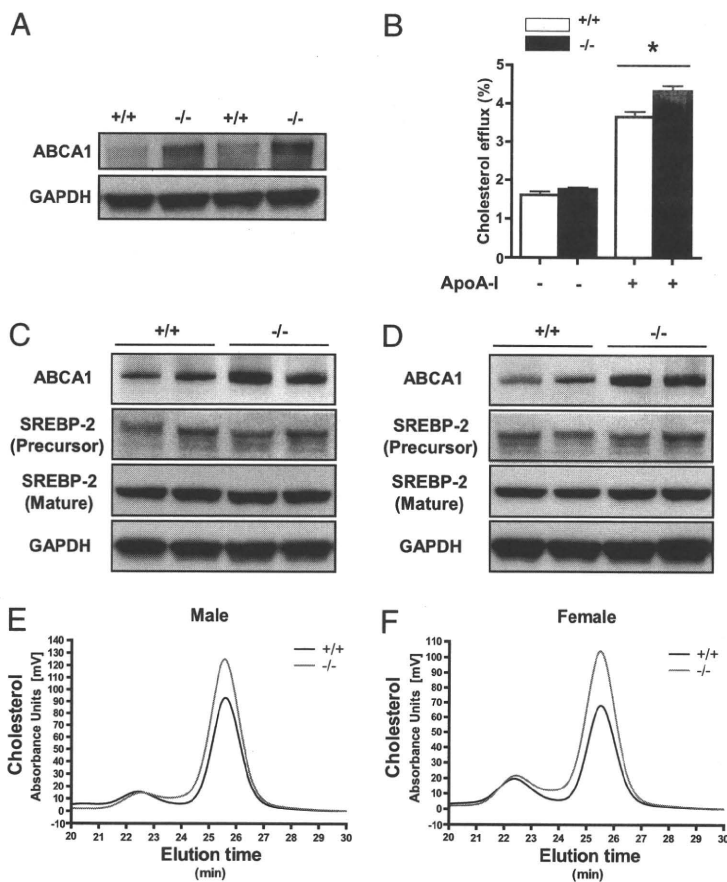


Fig. 5. ABCA1 expression of peritoneal macrophages and liver in WT and miR-33-deficient mice. (A) Western blot analysis of ABCA1 in peritoneal macrophages. Thioglycolate-elicited peritoneal macrophages were isolated from 8-wk-old WT and miR-33-deficient mice. GAPDH was used as a loading control. (B) Cholesterol efflux from peritoneal macrophages was measured in the presence or absence of apoA-I (15 $\mu\text{g}/\text{mL}$) for 6 h. Values are mean \pm SE of six independent experiments. $*P < 0.01$. (C) Western blot analysis of hepatic ABCA1 and SREBP-2 in 16-wk-old male mice. GAPDH was used as loading control. (D) Western blot analysis of hepatic ABCA1 and SREBP-2 in 16-wk-old female mice. GAPDH was used as loading control. (E) Representative HPLC analysis of serum cholesterol from male WT and miR-33-deficient mice. (F) Representative HPLC analysis of serum cholesterol from female WT and miR-33-deficient mice.

Table 1. Serum lipid profiling of WT and miR-33-deficient mice

	Lipoprotein		Males		Females	
	Major (fraction no.) diameter	Subclass (fraction no.)	(+/+) n = 6	(-/-) n = 5	(+/+) n = 6	(-/-) n = 5
TC (mg/dL)			73.70 ± 3.39	85.90 ± 4.11*	58.56 ± 3.37	78.19 ± 4.41**
	CM (1, 2) >80 nm		0.13 ± 0.03	0.21 ± 0.07	0.09 ± 0.02	0.12 ± 0.03
	VLDL (3-7) 30-80 nm		4.89 ± 0.75	4.04 ± 0.75	3.82 ± 0.37	3.49 ± 0.24
	LDL (8-13) 16-30 nm		13.25 ± 0.48	13.31 ± 0.90	13.78 ± 0.53	17.89 ± 1.57*
		Large LDL (8)	2.16 ± 0.13	2.31 ± 0.29	2.76 ± 0.23	3.10 ± 0.32
		Medium LDL (9)	4.32 ± 0.15	4.05 ± 0.22	4.90 ± 0.23	5.95 ± 0.68
		Small LDL (10)	3.27 ± 0.22	2.86 ± 0.16	3.12 ± 0.12	4.02 ± 0.40*
		Very small LDL (11-13)	3.51 ± 0.20	4.09 ± 0.51	2.99 ± 0.31	4.82 ± 0.46*
	HDL (14-20) 8-16 nm		55.42 ± 2.82	67.55 ± 4.09*	40.88 ± 3.22	56.69 ± 3.82*
		Very large HDL (14, 15)	3.85 ± 0.24	5.77 ± 0.64*	3.60 ± 0.66	5.97 ± 0.71*
		Large HDL (16)	16.50 ± 0.88	22.15 ± 1.35**	14.81 ± 1.79	21.04 ± 1.81*
		Medium HDL (17)	22.01 ± 1.18	25.65 ± 1.39	14.50 ± 0.73	19.57 ± 1.19**
		Small HDL (18)	9.24 ± 0.52	9.61 ± 0.63	5.30 ± 0.05	6.70 ± 0.33**
		Very small HDL (19, 20)	4.75 ± 0.19	5.12 ± 0.30	3.24 ± 0.09	3.60 ± 0.42
TG (mg/dL)			45.87 ± 6.20	37.26 ± 4.90	20.70 ± 2.64	20.64 ± 1.67

Values are mean ± SE. Blood was obtained from chow-fed 16-wk-old mice after a 4-h fast. Serum was analyzed by HPLC, as described in *Materials and Methods*. CM, chylomicrons; TC, total cholesterol; TG, triglyceride.

* $P < 0.05$, ** $P < 0.01$ compared with WT mice.

levels as compared with those in control mice fed a high-fat diet (15). Another report showed that overexpression of antisense miR-33 using lentivirus showed a 50% increase in hepatic ABCA1 protein levels and a concomitant 25% increase in plasma HDL levels after 6 d (14). Marquart et al. indicated that injection of an anti-miR-33 oligonucleotide resulted in a substantial increase in ABCA1 expression and HDL levels (16).

Antisense inhibition of miRNA function has been an important tool for elucidating miRNA biology. However, to determine the potential developmental functions and perform longer term studies, it is necessary to completely ablate the miRNA under investigation. We generated mice lacking miR-33, encoded by an intron of the *Srebp2*. The major findings obtained by the analysis of miR-33-deficient mice were that (i) mice homozygous for the miR-33 deletion were born at the expected Mendelian ratio, were viable, fertile, and did not display obvious abnormalities in size, shape, or structure up to 16 wk of age; (ii) complete loss of miR-33 enhanced liver ABCA1 protein levels remarkably, and serum HDL levels were elevated by ≈22% in male and 39% in female mice, probably because the expression level of miR-33 was 1.5-fold higher in the liver of female mice compared with male mice; (iii) the increased levels of HDL were composed mainly of very large, large, and medium HDL (mature HDL), which was consistent with the results obtained in *hABCA1* transgenic mice (25); and (iv) although the *in vitro* experiment suggested that *Abcg1* is also a potential target of miR-33, the depletion of miR-33 did not alter the expression levels of ABCG1 protein in liver. Rayner et al. could also not see the difference in hepatic ABCG1 protein expression levels between mice 6 d after injection with control and anti-miR-33 lentivirus (14). Thus, our results unambiguously indicated that miR-33 regulates plasma HDL levels through the repression of ABCA1 *in vivo*.

Gene regulation via miRNAs is a strongly conserved mechanism found in nearly all multicellular organisms, including animals and plants (26). Mammalian genomes encode more than 500 known miRNA genes. Approximately 50% are expressed from non-protein-coding transcripts, whereas the rest are located mostly in the introns of genes (27). Intronic miRNAs are generally transcribed coincidentally with their host genes (28). In the present study we showed the presence of miR-33 within the intronic sequence in the *Srebp2* gene and examined whether miR-33 is expressed with its host gene. *In vitro* studies demonstrated that *Srebp2* intron 16

suppressed ABCA1 protein expression in the same way as miR-33. The coregulation of a miRNA with its host gene typically exhibits one of two main functions: (i) an antagonistic effect by miRNA mediated knock-down of genes with perturbing effects on a pathway or a biological process activated by the host gene, or (ii) a synergistic effect by miRNA-mediated fine tuning of a target gene generating a positive effect on the host gene. In this case, miR-33 has a synergistic effect on ABCA1 via its host gene *Srebp2* because SREBP-2 is known to suppress the transcription of *Abca1* in vascular endothelial cells (29). SREBPs are activated in sterol-depleted conditions and serve as transcription factors for lipid/cholesterol synthesis, uptake, storage, and efflux (11-13, 29). In peripheral cells, intracellular cholesterol homeostasis is precisely regulated and depends on the balance among cholesterol synthesis, degradation, cholesterol ester formation, influx, and efflux (30, 31). Because SREBPs are activated by HMG-CoA reductase inhibitor accompanied by an increased in the expression of miR-33, ABCA1 expression and cholesterol efflux are presumably suppressed by miR-33 in these conditions.

In humans, *SREBP1* and *SREBP2* encode miR-33b and miR-33a, respectively (15). It is well known that hypertriglyceremia in metabolic syndrome is caused by the insulin-induced increase in *SREBP1c* mRNA and protein levels (32, 33). Low HDL often accompanies this situation, and it is possible that the reduction in HDL is caused by a decrease in ABCA1, because of the increased production of miR-33b from the insulin-induced induction of *SREBP1c*. Although it is impossible to prove this in animal models that lack miR-33b, antagonizing miR-33 could be a promising way to raise HDL levels when the transcription of both *SREBPs* is up-regulated. Thus, our study suggests that a combination of silencing of endogenous miR-33 and statins may be a useful therapeutic strategy for raising HDL and lowering LDL levels, especially for individuals with metabolic syndrome.

Materials and Methods

Cells and Plasmids. Immortalized human primary hepatocyte Hu5-E/2 cells were as described previously (17). Other cells and plasmids used in this experiment are summarized in *SI Materials and Methods*.

Generation of miR-33-Deficient Mice. A targeting vector was constructed by modifying bacterial artificial chromosome RP24-291F2 (Invitrogen) using defective prophage λ -Red recombination system (34, 35). As a selection marker,

a neomycin resistance cassette flanked by loxP sites (loxP-PGK-gb2-neo-loxP cassette; Gene Bridges) was inserted at the premiR-33 site. The targeting vector was electroporated into C57BL/6 mouse ES cells (DS Pharma Biomedical) using a Nucleofector system (Lonza). Positive clones were selected by incubating cells with 200 mM geneticin (Invitrogen) for 5 d, and homologous recombination was confirmed by Southern blotting. Successfully recombined ES cells were injected into blastocysts from ICR strain mice supplied by Unitech Inc, and chimeric mice were bred with C57BL/6 mice to generate F1 mice. The genotype of F1 mice was confirmed by Southern blotting. The neomycin resistance cassette was removed in the mouse germ line by breeding heterozygous mice with *Ayu-1* Cre knockin mice, which express Cre recombinase in multiple tissues, including the germ line (36). Descendant miR-33 heterozygous mice without the *Ayu-1* Cre allele were crossed with each other to generate miR-33-deficient mice. All experiments were carried out in C57BL/6 background mice, and WT littermates were used as a control. Primer sequences for the probe (865 bp) for Southern blotting and genotyping (WT, 385 bp, KO, 491 bp) are indicated in *SI Materials and Methods*.

Lentivirus Production and DNA Transduction. We produced lentiviral stocks in 293FT cells in accordance with the manufacturer's protocol (Invitrogen). Cells were used for analyses 2 d after transduction.

Luciferase Assay. To create WT or mutant 3'UTR luciferase reporter constructs, a fragment of the 3'UTR of the *Abca1* and *Abcg1* genes (*SI Materials and Methods*) was subcloned downstream of a CMV-driven firefly luciferase

cassette in a pMIR-REPORT vector (Ambion). Luciferase activities were measured as described previously (37).

Cellular Cholesterol Efflux from Macrophages. Cellular cholesterol efflux via apoA-I was determined as described previously (38).

Serum Lipid Profiling. Lipoproteins were analyzed by HPLC at Skylight Biotech (Akita, Japan), in accordance with the procedure described by Usui et al. (24).

Statistical Analysis. Data are presented as mean \pm SE. Statistical comparisons were performed using unpaired two-tailed Student *t* tests or one-way ANOVA with Bonferroni post hoc test where appropriate, with a probability value of <0.05 taken to indicate significance.

ACKNOWLEDGMENTS. We thank Naoya Sowa for providing excellent technical assistance; Neal G. Copeland (Institute of Molecular and Cell Biology, Singapore) for the defective prophage λ -Red recombination system; Junji Takeda (Osaka University, Osaka, Japan) and Kosuke Yusa (Osaka University, Osaka, Japan) for the plasmid used for the construction of the targeting vector; Ken-ichi Yamamura (Kumamoto University, Kumamoto, Japan) and Kimi Araki (Kumamoto University) for *Ayu-1* Cre-expressing mice; and Makoto Hijikata (Institute for Virus Research, Kyoto University, Kyoto, Japan) for HuS-E/2. This work was supported in part by grants from the Global COE program "Center for Frontier Medicine," from the Japan Society for the Promotion of Science, and from the Ministry of Education, Culture, Sports, Science, and Technology of Japan (to T. Kimura, T. Kita, K.H., T.H., and K.O.).

- Tall AR, Wang N (2000) Tangier disease as a test of the reverse cholesterol transport hypothesis. *J Clin Invest* 106:1205–1207.
- Francis GA, Knopp RH, Oram JF (1995) Defective removal of cellular cholesterol and phospholipids by apolipoprotein A-I in Tangier disease. *J Clin Invest* 96:78–87.
- Schmitz G, Langmann T (2001) Structure, function and regulation of the ABC1 gene product. *Curr Opin Lipidol* 12:129–140.
- Brooks-Wilson A, et al. (1999) Mutations in ABC1 in Tangier disease and familial high-density lipoprotein deficiency. *Nat Genet* 22:336–345.
- Bodzioch M, et al. (1999) The gene encoding ATP-binding cassette transporter 1 is mutated in Tangier disease. *Nat Genet* 22:347–351.
- Rust S, et al. (1999) Tangier disease is caused by mutations in the gene encoding ATP-binding cassette transporter 1. *Nat Genet* 22:352–355.
- Clee SM, et al. (2000) Age and residual cholesterol efflux affect HDL cholesterol levels and coronary artery disease in ABCA1 heterozygotes. *J Clin Invest* 106:1263–1270.
- Wang Y, Oram JF (2002) Unsaturated fatty acids inhibit cholesterol efflux from macrophages by increasing degradation of ATP-binding cassette transporter A1. *J Biol Chem* 277:5692–5697.
- Brown MS, Goldstein JL (1997) The SREBP pathway: Regulation of cholesterol metabolism by proteolysis of a membrane-bound transcription factor. *Cell* 89:331–340.
- Horton JD, et al. (1998) Activation of cholesterol synthesis in preference to fatty acid synthesis in liver and adipose tissue of transgenic mice overproducing sterol regulatory element-binding protein-2. *J Clin Invest* 101:2331–2339.
- Brown MS, Goldstein JL (1999) A proteolytic pathway that controls the cholesterol content of membranes, cells, and blood. *Proc Natl Acad Sci USA* 96:11041–11048.
- Shimano H, et al. (1996) Overproduction of cholesterol and fatty acids causes massive liver enlargement in transgenic mice expressing truncated SREBP-1a. *J Clin Invest* 98:1575–1584.
- Horton JD, Shimomura I (1999) Sterol regulatory element-binding proteins: Activators of cholesterol and fatty acid biosynthesis. *Curr Opin Lipidol* 10:143–150.
- Rayner K, et al. (2010) miR-33 contributes to the regulation of cholesterol homeostasis. *Science* 328:1570–1573.
- Najafi-Shoushtari SH, et al. (2010) MicroRNA-33 and the SREBP host genes cooperate to control cholesterol homeostasis. *Science* 328:1566–1569.
- Marquart TJ, Allen RM, Ory DS, Baldan A (2010) miR-33 links SREBP-2 induction to repression of sterol transporters. *Proc Natl Acad Sci USA* 107:12228–12232.
- Aly HH, et al. (2009) Strain-dependent viral dynamics and virus-cell interactions in a novel in vitro system supporting the life cycle of blood-borne hepatitis C virus. *Hepatology* 50:689–696.
- Wang D, et al. (2009) Cepred: Predicting the co-expression patterns of the human intronic microRNAs with their host genes. *PLoS ONE* 4:e4421.
- Kim YK, Kim VN (2007) Processing of intronic microRNAs. *EMBO J* 26:775–783.
- Shimano H, et al. (1997) Elevated levels of SREBP-2 and cholesterol synthesis in livers of mice homozygous for a targeted disruption of the SREBP-1 gene. *J Clin Invest* 100:2115–2124.
- Basso F, et al. (2003) Role of the hepatic ABCA1 transporter in modulating intrahepatic cholesterol and plasma HDL cholesterol concentrations. *J Lipid Res* 44:296–302.
- Timmins JM, et al. (2005) Targeted inactivation of hepatic *Abca1* causes profound hypoalphalipoproteinemia and kidney hypercatabolism of apoA-I. *J Clin Invest* 115:1333–1342.
- Okazaki M, et al. (2005) Identification of unique lipoprotein subclasses for visceral obesity by component analysis of cholesterol profile in high-performance liquid chromatography. *Arterioscler Thromb Vasc Biol* 25:578–584.
- Usui S, Hara Y, Hosaki S, Okazaki M (2002) A new on-line dual enzymatic method for simultaneous quantification of cholesterol and triglycerides in lipoproteins by HPLC. *J Lipid Res* 43:805–814.
- Vaisman BL, et al. (2001) ABCA1 overexpression leads to hyperalphalipoproteinemia and increased biliary cholesterol excretion in transgenic mice. *J Clin Invest* 108:303–309.
- Carrington JC, Ambros V (2003) Role of microRNAs in plant and animal development. *Science* 301:336–338.
- Saini HK, Griffiths-Jones S, Enright AJ (2007) Genomic analysis of human microRNA transcripts. *Proc Natl Acad Sci USA* 104:17719–17724.
- Ying SY, Lin SL (2006) Current perspectives in intronic micro RNAs (miRNAs). *J Biomed Sci* 13:5–15.
- Zeng L, et al. (2004) Sterol-responsive element-binding protein (SREBP) 2 down-regulates ATP-binding cassette transporter A1 in vascular endothelial cells: A novel role of SREBP in regulating cholesterol metabolism. *J Biol Chem* 279:48801–48807.
- Hayden MR, et al. (2000) Cholesterol efflux regulatory protein, Tangier disease and familial high-density lipoprotein deficiency. *Curr Opin Lipidol* 11:117–122.
- Fielding CJ, Fielding PE (1997) Intracellular cholesterol transport. *J Lipid Res* 38:1503–1521.
- Kim JB, et al. (1998) Nutritional and insulin regulation of fatty acid synthetase and leptin gene expression through ADD1/SREBP1. *J Clin Invest* 101:1–9.
- Chen G, Liang G, Ou J, Goldstein JL, Brown MS (2004) Central role for liver X receptor in insulin-mediated activation of *Srebp-1c* transcription and stimulation of fatty acid synthesis in liver. *Proc Natl Acad Sci USA* 101:11245–11250.
- Copeland NG, Jenkins NA, Court DL (2001) Recombineering: A powerful new tool for mouse functional genomics. *Nat Rev Genet* 2:769–779.
- Horiguchi M, et al. (2009) Fibulin-4 conducts proper elastogenesis via interaction with cross-linking enzyme lysyl oxidase. *Proc Natl Acad Sci USA* 106:19029–19034.
- Morita M, et al. (2003) HLF/HIF-2 α is a key factor in retinopathy of prematurity in association with erythropoietin. *EMBO J* 22:1134–1146.
- Nishi H, et al. (2010) MicroRNA-15b modulates cellular ATP levels and degenerates mitochondria via Arl2 in neonatal rat cardiac myocytes. *J Biol Chem* 285:4920–4930.
- Zhang Z, et al. (2001) Expression of cholesterol ester transfer protein in human atherosclerotic lesions and its implication in reverse cholesterol transport. *Atherosclerosis* 159:67–75.

遺伝子医学MOOK 別冊

はじめての 臨床応用研究

別 刷

株式会社メディカルドゥ

3. 知っておきたい臨床応用への制度： 高度医療と先進医療

村山敏典・横出正之

臨床応用研究の最終目標の1つは、先端医療技術の安全性と有効性を科学的に評価して、健康保険が使える標準医療として患者のもとに迅速に届けることだが、臨床試験を行う際にも、試験中の医療費の取り扱いや試験費用の負担区分に配慮する必要がある。わが国ではいわゆる混合診療が禁止されており、研究的な医療と一般医療を同時に行う場合には、国が承認する「治験」または「先進医療」という制度のもとで実施しないかぎり、健康保険が併用できない。本稿では、先進医療とその類型である高度医療評価制度について説明する。

Key words

先進医療，高度医療，高度先進医療，治験，いわゆる混合診療

はじめに

今から半世紀以上前の1957年に「保険医療機関及び保険医療養担当規則」（以下、療養担当規則）という省令が当時の厚生省から出され、その第18条には「保険医は、特殊な療法又は新しい療法等については、厚生大臣の定めるもののほか行ってはならない」と定められた。これが、論議が繰り返されてきたいわゆる混合診療禁止の根拠となる法令であって、研究段階の医療と一般診療を併用する場合には、国が定める例外を除き、一般診療部分にも健康保険が適用されず、全体が自由診療となる。それでは、国はどのような場合に健康保険の併用を認めているのだろうか。高度先進医療、高度医療、先進医療とよく似た名前の制度があるが、この違いは何だろうか。

現在、研究段階の医療で健康保険診療が併用できるものは、治験と先進医療（後述の高度医療を含む）の2種類に限られている。治験とは、Good Clinical Practice (GCP) と呼ばれる国際的な統一ルールや薬事法などに基づいて、医薬品・医療機器の製造販売の承認申請の資料を収集するための臨床試験である。従来企業主導治験に加えて、2003年からはわが国でも医師・研究者主導の治験を行うことが可能になった。未承認あるいは適応外の医薬品・医療機器の薬事承認を受けるためには、治験を行うことが大原則だが、本稿ではその説明は省略する。

I. 高度先進医療（1984～2006）

1984年に上記の療養担当規則が改正され、高度先進医療という制度が開始された。これにより、質的・量的に高水準の医療基盤をもつ大学病院などの医療機関を「特定承認保険医療機関」と認定し、これらの医療機関で実施される場合にかぎり、特定の医療技術を高度先進医療として健康保険の併用を認め、保険診療該当部分を特定療養費として健保組合が支給することになった。この制度は2006年まで存続し、約20年間で185種類の医療技術が高度先進医療として承認され、そのうち66種類が最終的に保険収載された。高度先進医療の中には、未承認あるいは適応外の医薬品・医療機器を用いる医療技術も含まれていた。高度先進医療の問題点として、審査に長期間を要していたこと、非公開の会議で審議過程が不明であったこと、何年も高度先進医療のままで保険医療に至らない医療技術も多かったことなどが挙げられる。

II. 先進医療（2005～）

そこで2004年12月に、規制改革・民間開放推進会議の答申を受けて、当時の尾辻厚生労働大臣と村上規制改革大臣の間で「いわゆる「混合診療」問題に係る基本的合意」^{HP1}がなされ、2005年7月から「先進医療」制度が開始された。有効性および安全性を確保する視点から、医療技術ごとに一定の施設基準を設定し、施設基準に該当する保険医療機関は届け出により先進医療として保険診療との併用が可能になった（図①）。2010年9月現在、87種類の先進医療が認められている。

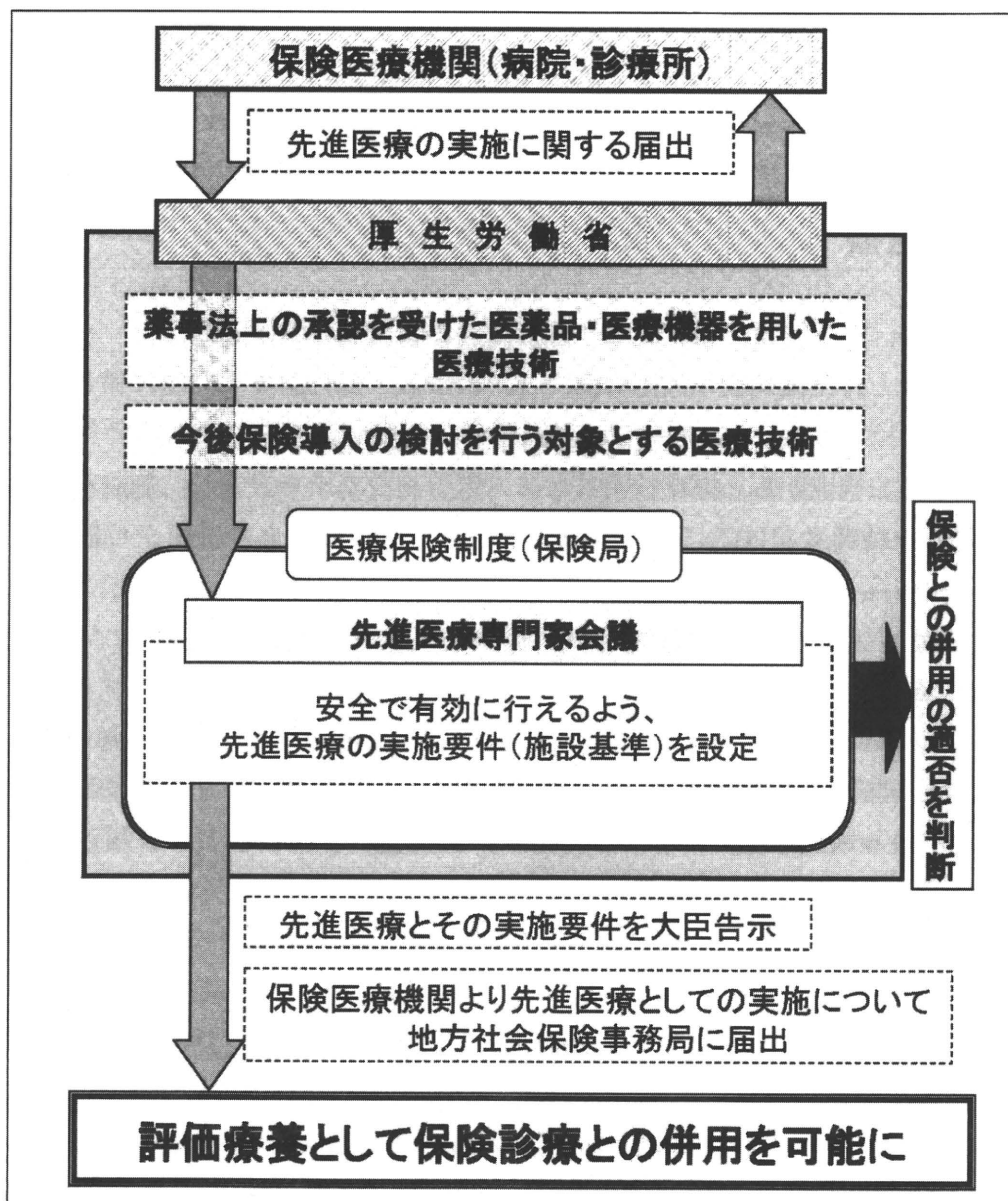
「厚生労働大臣の定める先進医療及び施設基準」（先進医療告示^{HP2}）という告示の第2項に先進医療の基準が書かれているので、第2項先進医療とも呼ばれる。先進医療では、未承認あるいは適応外の医薬品・医療機器を用いる医療技術は取り扱わない（図②）。既に承認された医薬品・医療機器を、定められた用量・用法・効能・効果の範囲内で用いる医療技術なので、画像診断、IT、遺伝子診断などを併用した医療技術が多く承認されている。2006年10月の健康保険法改正により、22年間続いた高度先進医療が廃止され、先進医療に一本化されたが、高度先進医療に一部含まれていた未承認・適応外医薬品/医療機器を用いる医療技術は、いったん時限的先進医療として継続の可否を評価されたあと、最終的に後述の高度医療に引き継がれた。

先進医療を含む医療費の負担区分を図③に示す。先進医療に係る費用は全額患者の自己負担となり、それ以外の通常の治療と共通する部分（診察・検査・投薬・注射・入院料など）は、一般の保険診療と同じように扱われる。図の例では、先進医療部分

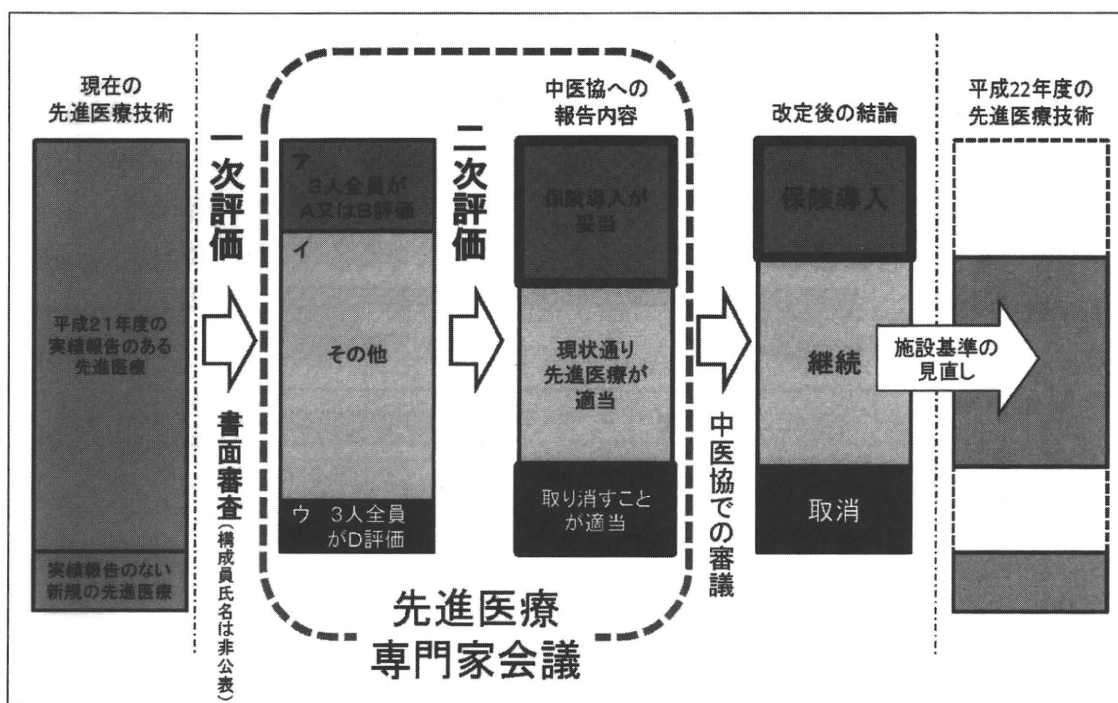
が20万円で全額が患者自己負担, 一般診療相当の80万円の3割自己負担が24万円で, 患者の自己負担分合計は44万円, ただし保険給付自己負担分については高額療養費制度が適用されるが, 先進医療部分には適用されない。実際には先進医療部分がさらに高額となるものも多く, 多くの保険会社が先進医療部分の医療費を補償する特約保険商品売り出している。

先進医療の相談窓口は厚労省保険局医療課で, 新規申請の場合には, 保険医療機関の開設者(大学病院の場合は学長など)が, 先進医療届出書以下, 十数種類の書類と定められた文献3本以上を, 地方厚生局長を通じて厚生労働大臣に提出する^{HP3}。提

図① 第2項先進医療に係る取り扱いについて(ホームページ4より)



図④ 平成22年度診療報酬改定に向けた先進医療の保険導入等及び施設基準の見直しに係る検討方法について
(ホームページ3より)



たものとし、その翌月より（受理日が初日の場合は当月より）、保険診療との併用が可能になる。なお、前年7月から当該年6月までの間に行った先進医療の実績は8月末までに地方厚生局長に報告する必要がある。また、先進医療による副作用などで死亡またはそれに準じて重篤な症例は発生より7日以内に、その他重篤未知の副作用は発生より15日以内に、地方厚生局長および厚生労働大臣に報告する必要がある。さらに、重要な研究報告や海外での規制措置などの健康危険情報を入手した場合にも地方厚生局長および厚生労働大臣に報告する必要がある。これらの義務は、治験で運用されている国際ルールとほぼ同じものである。

先進医療技術は、毎年先進医療専門家会議で実績報告を受け、2年に1回の診療報酬改定の前に、この会議で有効性・安全性・技術的成熟度・社会的妥当性・普及性・効率性を評価し、保険導入について検討される（図④）。

Ⅲ. 高度医療（2008～）

高度先進医療から先進医療に移行した後、従来は高度先進医療で受け付けられていた薬事法上未承認・適応外の医薬品・医療機器を用いる医療技術が、新たに先進医療として申請され、事務局で先進医療では取り扱わないとして却下される例が相次いだ。

そこで、2008年4月に先進医療の枠を拡大して、新たに第3項先進医療（先進医療告示の第3項に基準を記載）として高度医療評価制度が創設された（図②）。医学医療の高度化やこれらの医療技術を受けたいという患者のニーズなどに対応するため、薬事法の承認などが得られていない医薬品・医療機器の使用を伴う先進的な医療技術を、一定の要件の下に「高度医療」として認め、保険診療と併用できることとし、薬事法上の承認申請などにつながる科学的評価可能なデータ収集の迅速化を図ることが目的とされている。ただし、高度医療のデータを治験の計画根拠に使用することはできるが、このデータだけでは薬事承認を得られないので、研究者や企業などの開発方針にもよるが、もし治験として実施することが可能であるならば当初から治験をめざすほうが最終的には標準医療導入への早道となる。高度医療の申請の際には、どのように医療開発を進めるかという具体的なロードマップを国に提示する必要がある。

2010年9月現在、高度医療（第3項先進医療）として29種類が承認されているが、高度先進医療の時代から引き継がれた14種類を除くと、高度医療評価制度創設以後に新たに認められたものは15種類である。当初は国内外未承認医薬品・医療機器の対応を巡って議論がされていたが、高度医療評価会議で一定の見解が示されてからは比較的円滑に審議が進んでいる。

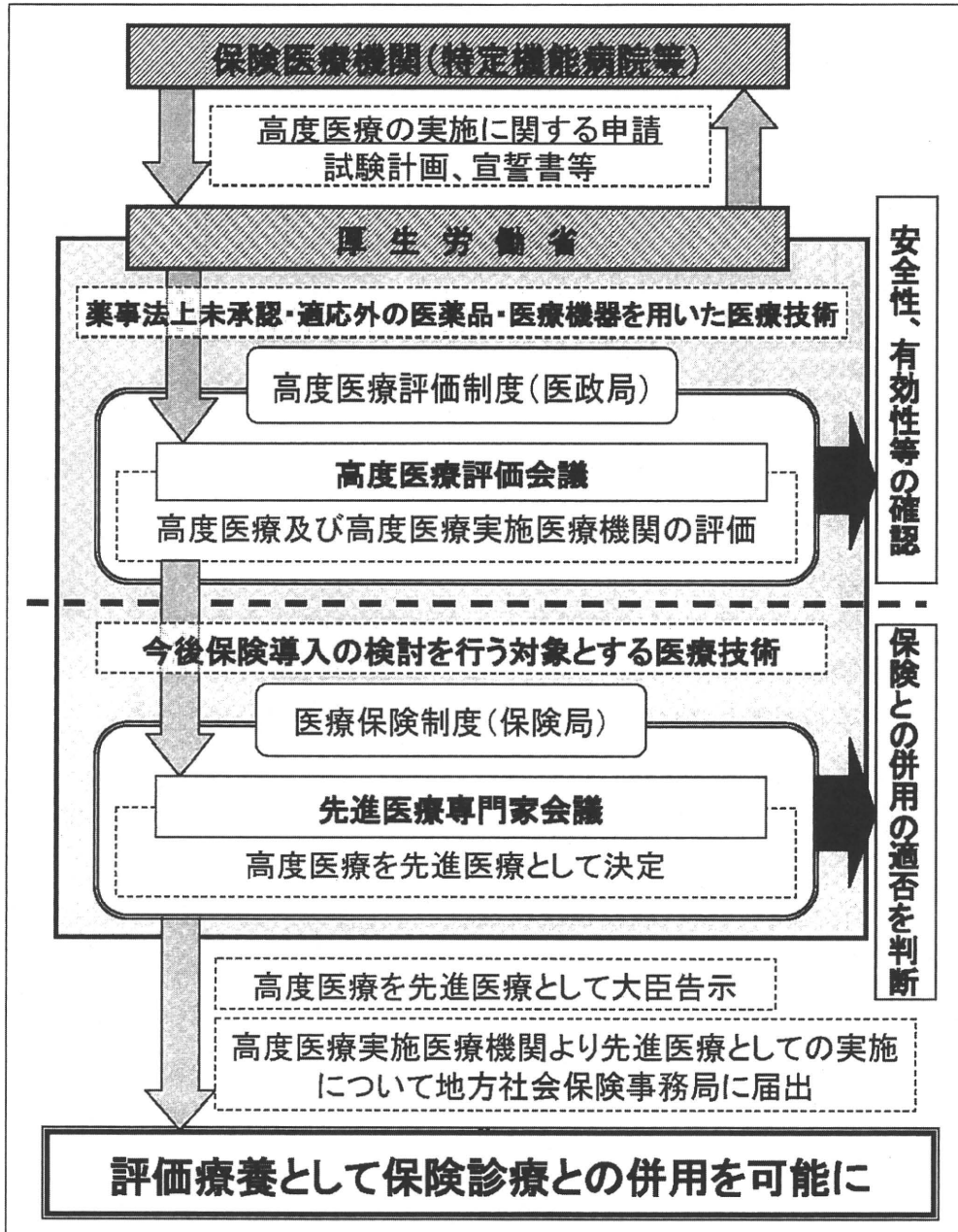
高度医療は第3項先進医療と呼ばれるとおりに先進医療の類型ではあるが、その相談窓口は先進医療とは異なり、厚労省医政局研究開発振興課となっている。高度医療の新規申請にあたっては、医療機関の開設者が、高度医療実施申請書以下、十数種類の書類と定められた文献2本以上を医政局長に提出する^{HP4}。高度医療評価会議で医療技術の安全性・科学性が評価されたあと、先進医療専門家会議に送付され、そこで保険併用の可否を審議される（図⑤）。同会議以降のプロセスは前項で述べたものと同じである。

なお高度医療はプロトコルに基づく純然たる臨床試験だが、その実施にあたり、「臨床研究に関する倫理指針」などの遵守に加え、以下のような要件が課せられている。

- ①特定機能病院に相当する医療体制
- ②データマネジメント体制の確保
- ③多施設共同研究の際にはモニタリング体制の確保
- ④国への副作用報告（7日、15日）、健康危険情報報告（先進医療と同じ）
- ⑤国への定期報告、終了報告（先進医療と同じ）
- ⑥事前通告のない立入り調査

データマネジメントやモニタリングについて、具体的にどのような体制を整備すべきかについては、高度医療評価会議でも議論はされていないが、少なくとも「臨床研究に関する倫理指針」に沿って行われる通常の臨床試験よりは、高度の医療体制と臨

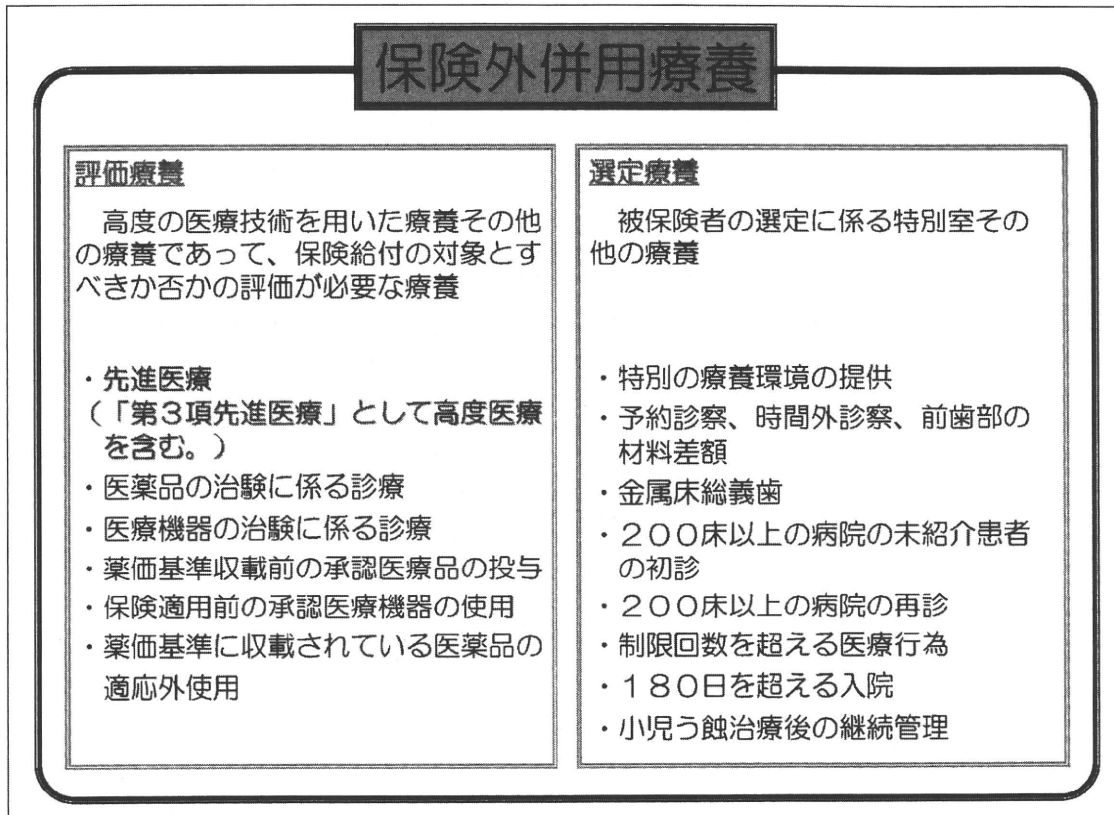
図⑤ 第3項先進医療（高度医療）に係る取り扱いについて（ホームページ4より）



床試験実施・支援体制が要求されている。

おわりに

臨床応用への制度として、国に届け出をして承認を受ける必要のある先進医療と高度医療（第3項先進医療）について、その概要を述べた。どちらも、保険診療との併

図⑥ 保険外併用療養^{用解1}（ホームページ4より）

用が可能な制度であり、臨床応用研究を進める際に検討すべき選択肢の1つである。未承認または適応外の医薬品・医療機器を用いる医療技術は高度医療の範疇となるが、そこで得られたデータは治験実施計画立案の根拠に用いられることはあっても、通常はこのデータだけでは薬事承認を申請することはできない。常に5年後、10年後を見越して、どのように臨床展開をめざしていくかをプロジェクトとして考え続けることが極めて重要である。

用語解説

1. **保険外併用療養費（図⑥）**：健康保険法が2006年に改正され、それまでの特定療養費制度に代わり、保険外併用療養費が導入された。わが国では、いわゆる混合診療が禁止されているため、健康保険が適用されない保険外診療を受けるときには、保険診療部分も含めて医療全体が自由診療（患者自己負担または研究者負担）となる。

ただし、保険外診療を受ける場合でも、厚生労働大臣の定める「評価療養」と「選定療養」については、保険診療との併用が認められており、通常の治療と共通する部分（診察・検査・投薬・入院料など）の費用は、一般の保険診療と同様に扱われ、その部分については患者が2～3割の自己負担金を支払い、残りの額は「保険外併用療養費」として健康保険組合から給付される。

「評価療養」とは、医学的な評価が定まっていない新しい治療法など、将来的に保険給付